

CHAPTER 188

OBSERVATION OF FORESHORE VARIATION IN IWO-JIMA

By Toshiyuki Shigemura¹, Member, ASCE,
Kenjiro Hayashi¹ and Koji Fujima¹

Abstract

The variation of the foreshore in Iwo-jima is studied by analyzing a series of aerial photographs taken seasonally for the past 4 years since 1987, and data of various surveys obtained for the past 10 years since 1982. These observations are compared with results of numerical analysis of the effects of storm waves on the foreshore. The findings obtained through these analyses are: (1)The island is still rising at a yearly rate of more than 30 cm/year; (2)The foreshore is eroded in summer and fall when typhoons often hit the island, but is restored back in winter and spring of the following year. The seasonal variation of the foreshore area ranges from 300,000 m² to 600,000 m² depending on the magnitude and frequency of the typhoons hitting the island in a year; (3)The foreshore area is increasing at a rate of 50,000 m²/year which is caused by the upheaval of the island; (4)A one-line model can be applicable for the prediction of the short-term variation of the shoreline caused by storm waves.

1. Introduction

Iwo-jima is an isolated volcanic island located in the Pacific Ocean about 1250 km south of Tokyo (24°45' to 24°49'N, 141°17' to 141°21'E). Figure 1 shows the location of the island.

The maximum length of the island is about 8.6 km and its surface area is roughly 23.2 km². The island is relatively flat with a mean altitude of 110 m and its surface is covered with dense vegetation.

The coast is mostly rimmed by a uniform sandy beach approximately 200 m wide, fully exposed to the open sea. Since the island often experiences typhoons in summer and fall, the seasonal variation of the foreshore is quite remarkable. Further, the island has

¹ Department of Civil Engineering, National Defense Academy,
1-10-20 Hashirimizu, Yokosuka, Kanagawa 239 JAPAN

been rising at an unusual rate of more than 30 cm/year in some places, making the variation of the foreshore more complicated. These environmental conditions have prevented us from constructing any operative port facilities in this island.

To investigate the mechanisms by which the foreshore changes, the authors have been conducting various surveys on the shore of the island since 1982, and have been taking aerial photographs since 1987.

This paper intends to clarify the following items through the analysis of these field data:

- (1) The current state of the rate of upheaval of the island.
- (2) The seasonal variation of the foreshore.
- (3) The effect of upheaval on the increase of foreshore area.
- (4) The mechanism by which the foreshore changes due to storm waves.

2. Field surveys and Aerial Photographs

(1) Field surveys on the shore of Iwo-jima

To investigate the variation of the rate of upheaval, the authors have been conducting traverse, level and cross surveys on the shore of Iwo-jima since 1982, with the support of the Topographic Survey Battalion(TSB) of Japan Ground Self Defense Force(JGSDF). Figure 2 shows the location of 53 measuring points provided at an interval of roughly 300 m along the entire backshore of the island.

By using these measuring points, surveys have been carried out at a frequency of at least twice a year. So far, surveys have been conducted 16 times in the period between 1982 and 1991.

In this study, the results of the level and cross surveys will be analyzed to check the current rate of upheaval and the variation of the foreshore slope of the island.

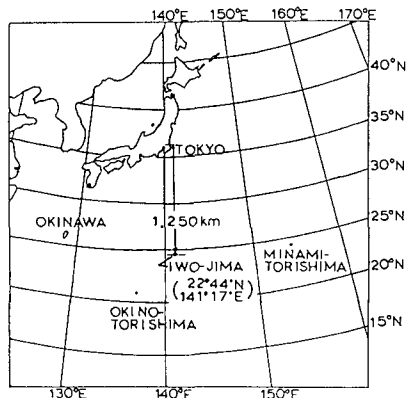


Figure 1 Location of Iwo-jima

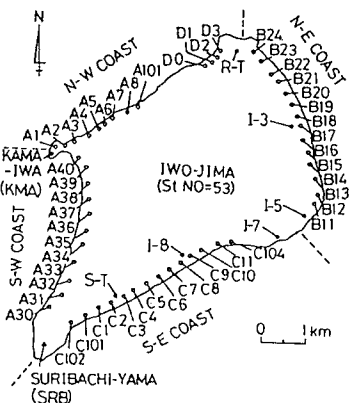


Figure 2 Location of measuring points

(2) Processing aerial photographs

To investigate the seasonal variation of the foreshore area, the authors have been taking aerial photographs of the island, seasonally since 1987, through the support of the Japan Maritime Self Defense Force (JMSDF). The photographs were taken vertically at an altitude of 3000 m, on three flight courses set in advance over the coast of the island. Photographs were taken at both low and high tides in each photographing operation, setting the overlapping rate to be 60%. Table 1 summarizes the details of the photographing operation.

From these photographs, mosaic maps of the island with a scale of 1/10000 were made with the aid of the TSB. So far, 15 sets of the mosaic maps have been completed. On each one, a common coordinate system was provided as shown in figure 3. Here, the X axis was placed along the runway heading in the ENE direction and the origin was placed at the western end of the runway.

Based on this coordinate system, the shoreline on each mosaic map was digitized at increments of 1 mm by using a special digitizer.

Table 1 Details of the photographing operation

No.	Date	Time	Tide (cm)
1	1987.04.24	1300-1400	60.0 (FLD)
	1987.04.24	1520-1610	81.0 (LHW)
2	1987.07.07	1548-1620	86.0 (HHW)
	1987.07.08	1030-1118	25.0 (LLW)
3	1987.10.28	0855-0912	70.0 (FLD)
	1987.10.28	1142-1150	86.0 (LHW)
4	1988.02.02	0700-0730	86.0 (LHW)
	1988.02.02	1210-1240	51.0 (HLW)
5	1988.04.07	0800-0837	64.0 (FLD)
	1988.04.07	1116-1132	68.0 (EBB)
6	1988.08.22	1531-1644	88.0 (LHW)
	1988.08.23	0853-0948	37.0 (LLW)
7	1988.10.25	0701-0729	106.0 (HHW)
8	1989.01.23	1322-1340	48.0 (HLW)
	1989.01.25	0836-0852	89.0 (HHW)
9	1989.04.20	1212-1313	20.0 (LLW)
	1989.05.15	0900-0940	83.0 (HHW)
10	1989.09.06	1523-1536	64.0 (HLW)
	1989.09.08	1203-1220	82.0 (LHW)
11	1989.11.07	1400-1430	87.0 (LHW)
	1989.11.08	0800-0830	38.0 (LLW)
12	1990.01.16	1608-1657	42.0 (HLW)
	1990.01.17	0941-1254	87.0 (FLD)
13	1990.05.18	1130-1240	76.0 (LHW)
	1990.05.19	0740-0802	53.0 (HLW)
14	1990.07.17	1424-1529	78.0 (EBB)
	1990.07.18	0837-0853	38.0 (LLW)
15	1991.05.23	1531-1610	78.0 (LHW)
	1991.05.24	0915-0936	34.0 (LLW)

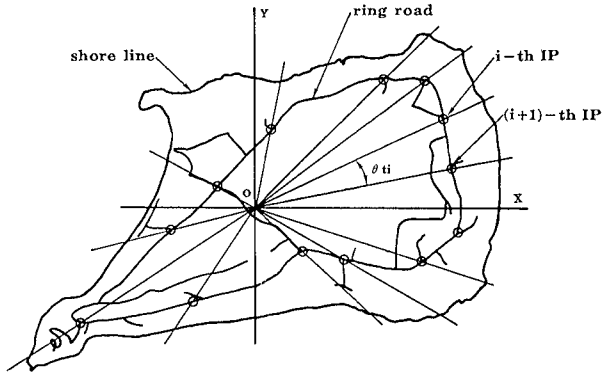


Figure 3 Coordinate system and inspection points provided for the data correction

(3) Correction of shoreline data

Shoreline data digitized from aerial photographs may include some errors caused either by mishandling of the camera during the photography, or by the incompleteness of the mosaic. Corrections should therefore be made on each set of the shoreline data so that all the measurements should have equivalent reliability.

To carry out this correction, thirteen inspection points were selected along a road that encircled the island (see Figure 3). These points were chosen because they can be distinguished clearly on each mosaic map. They were also identified on a reference map with a scale of 1/10000, made by enlarging the latest topographical map of the island revised in 1982 by the Geographical Survey Institute of the Japanese Ministry of Construction.

The corrections to the shoreline data were performed through the following procedures in each subdivided area defined by two adjacent inspection points and the origin of the coordinate system:

(a) Superpose the origin of the subdivided area on a mosaic map on to the origin of the corresponding area on the reference map, as shown in figure 4(a).

(b) Rotate the shoreline data of the mosaic map so that the bisector of θ_{mi} lies on the bisector of θ_{ti} , where θ_{mi} is an angle determined by the i -th and the $(i+1)$ -th inspection points, and the origin of the coordinate on the mosaic map, and θ_{tm} is the corresponding angle determined on the reference map (see figure 4(b)).

(c) Make an angle correction on the shoreline data of the mosaic map so that θ_{mi} becomes equal to θ_{ti} . Divide both θ_{mi} and θ_{ti} into increments of 1 degree to determine the length of dividing lines, l_m and l_t , where l_m is the length from the origin to the intersection point of a dividing line with the ring road on the mosaic map, and l_t is the corresponding length on the reference map (see figure 4(c)).

(d) Determine the correction factors $r_{i,j}$ and $r_{i,j+1}$ on every dividing line within the i -th subdivided area, where $r_{i,j}$ is the

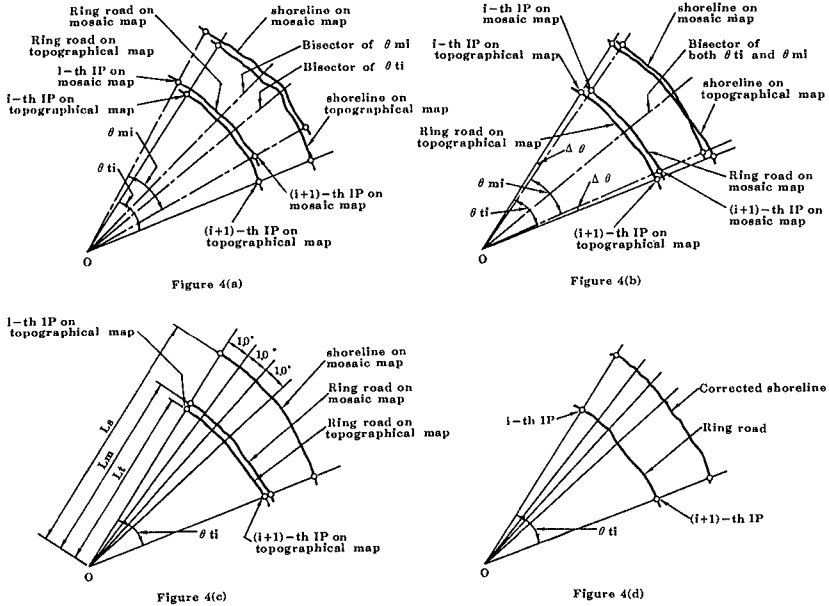


Figure 4 Correction procedures for eliminating the human errors on mosaic map

ratio l_t/l_m on the j -th dividing line, and $r_{i,j+1}$ is ratio l_t/l_m on the $(j+1)$ -th dividing line, both in the i -th subdivided area.

(e) Based on the values of $r_{i,j}$ and $r_{i,j+1}$, determine the correction factor r for any of the shoreline data in the area surrounded by the j -th and the $(j+1)$ -th dividing lines, and multiply each shoreline measurement of the mosaic map by r to get the corrected shoreline data (see figure 4(d)).

By performing this procedure on the original shoreline data, most of the human errors might possibly be eliminated.

However, these shoreline data, still include some errors caused by differences in tide level at the respective instants when the aerial photographs were taken. In order to eliminate this error, all of the shoreline data have to be adjusted to refer to a common level.

A datum plane (the Indian tide plane) was chosen as the reference level, and it was decided to reduce the shoreline data to this datum plane by using equations derived as follows:

Figure 5 shows a coordinate system used for the derivation of the equations. Suppose that A, B and C in this figure are points on the shoreline whose positions were digitized successively. Further, suppose that the photograph was taken when the tidal level was at an elevation η_t above the datum plane, and that the foreshore slope around these points is I_{fs} .

Now, we draw two lines at point B, one of them perpendicular to

the line AB and the other perpendicular to the line BC. Points $B_1'(X_1', Y_1')$ and $B_2'(X_2', Y_2')$ lie on these normals at the points where the elevation of the foreshore coincides with that of the datum plane. Their coordinates are determined as follows:

$$\begin{aligned}
 L &= \eta_t / I_{fs} & (1) \\
 X_1' &= X + L \sin \theta_1 & (2) \\
 Y_1' &= Y + L \cos \theta_1 & (3) \\
 X_2' &= X + L \sin \theta_2 & (4) \\
 Y_2' &= Y + L \cos \theta_2 & (5)
 \end{aligned}$$

Thus, the position of the point $B'(X', Y')$, the midpoint between B_1' and B_2' , can be determined by the following equations.

$$\begin{aligned}
 X' &= (X_1' + X_2') / 2 & (6) \\
 Y' &= (Y_1' + Y_2') / 2 & (7)
 \end{aligned}$$

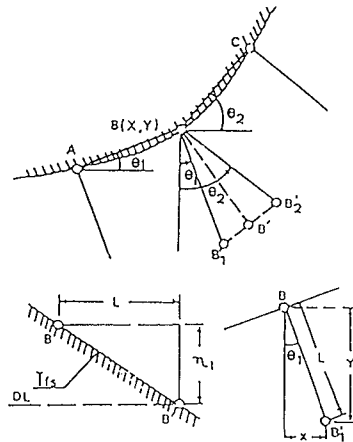


Figure 5 Coordinate system used to determine the shoreline data at the datum plane

By using these equations, errors due to the difference in tide level can also be eliminated from the shoreline data.

3. Results of the analyses

(1) Seasonal variation of foreshore slope

As stated in the preceding Chapter, the foreshore slope near the swash zone I_{fs} is needed for converting the shoreline data digitized from a mosaic map into one at the datum plane. To get this information, analyses were made on the results of cross surveys which have been done 16 times in the period between 1982 and 1991.

Figure 6 shows the seasonal variation of mean foreshore slope I_{fs} on each of the N-W, N-E, S-W and S-E coasts. Each coast was

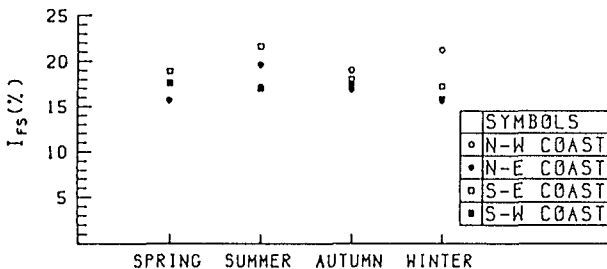


Figure 6 Seasonal variation of mean foreshore slope on each of the subdivided coasts

subdivided to obtain the local trend in the variation of foreshore slope and upheaval (see figure 2). The slopes used in reducing the corresponding shoreline data are the averages of all values of I_{fs} obtained at the measuring points on each coast.

The following facts were revealed through this analysis:

(a) Local values of I_{fs} vary in the range from 17 to 20% during summer and fall although they vary in the range from 15 to 19% during winter and spring.

(b) Local trends are not observed clearly in the seasonal variation of I_{fs} .

By using these values of I_{fs} , shoreline data were all converted to the datum plane.

(2) Current state of upheaval

To investigate the current state of upheaval in Iwo-jima, results of level surveys were analyzed intensively. Figure 7 shows the local variation of mean upheaval rate determined at measuring points on each coast. Here, the mean upheaval rate at each point means the rate determined by averaging the upheaval rates observed at the same point 16 times in the period from 1982 to 1991. All rates have been converted into cms per year. Further, the abscissa indicates the distance of each measuring point measured northward from the southernmost measuring point provided on each coast (see figure 2). Through this analysis, the following facts were found:

(a) The mean upheaval rate tends to increase towards the north.

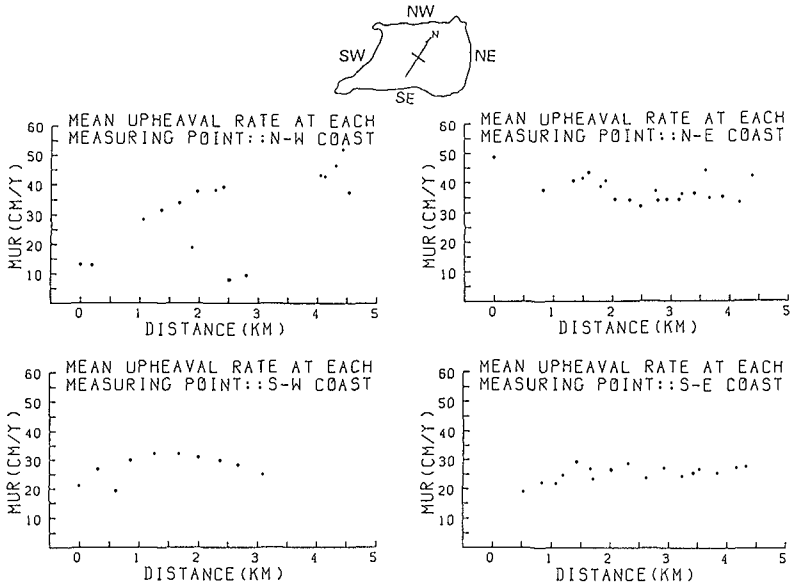


Figure 7 Mean upheaval rate at the measuring points on each of the subdivided coasts

(b) The mean upheaval rate is roughly 20 cm/year around the southern part of the island and 30 to 40 cm/year in the northern part of the island.

Tsuji et al (1969) have investigated the upheaval of Iwo-jima by comparing the elevations shown in a topographical map published by the US Army in 1952 with their surveyed data obtained in 1968. They revealed that the northern part of the island rose roughly 9 m in 16 years after 1952, while the southern part rose roughly 3 m in the same period. Further, Kosaka et al(1979) have analyzed old maps and charts of the island published prior to 1968, together with their own data surveyed in the next decade after 1968, and have reported that the island continued to rise at a rate of roughly 30 cm/year after 1952. Referring to these results, it can be concluded that the island is currently rising in the same way and at a similar rate to those revealed by earlier works.

(3) Seasonal variation of the foreshore area

Before checking the seasonal variation of the foreshore area in Iwo-jima, we look at the time history of the total surface area, which has increased steadily since 1911.

Figure 8 shows the history of the surface area determined by analyzing old maps, charts published after 1911, and mosaic maps described in the preceding Chapter. Among these data, those prior to 1986 were introduced in the authors' previous work (Shigemura et al, 1986).

Further, data determined from the mosaic maps are shown in the upper right of this figure within a dotted rectangle. From this figure, the following facts were revealed:

(a) Iwo-jima has continued to increase its surface area in the past 8 decades, although the rate of increase has been reduced slightly after 1980.

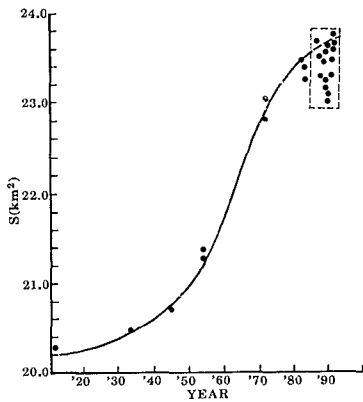


Figure 8 Time-history of the surface area of Iwo-jima after 1911

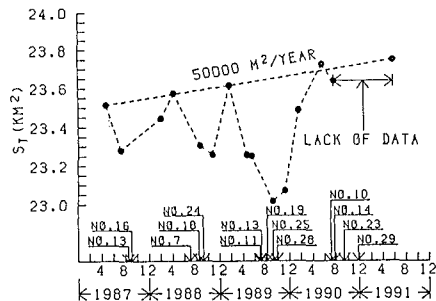


Figure 9 Seasonal variation of the surface area of Iwo-jima after 1987

(b) The envelope for the maximum area determined from the mosaic maps seems to lie on an extension of the curve through observations prior to 1980, although the seasonal variation of surface area is quite remarkable.

Now, we consider the seasonal variation of the foreshore area more closely. Figure 9 shows the seasonal variation of surface area determined by analyzing the mosaic maps. Here it should be noted that the seasonal variation of surface area may indicate that of the foreshore area itself. The numbers shown on the abscissa indicate the typhoons which passed within a range of 500 km from the island. From this figure, the following facts were revealed:

(a) The foreshore area is eroded in the period from summer to fall when typhoons often hit the island, but is restored in the period from winter to spring of the next year in which local waves of roughly 1 m high are predominant.

(b) The seasonal variation of the foreshore area ranges from 300,000 m² to 600,000 m², depending on the magnitude and frequency of typhoons which hit the island in a year.

(c) The foreshore area is currently increasing at a rate of roughly 50,000 m² per year, which might be caused by the upheaval of the island.

(4) Effect of the upheaval on the increase of foreshore area

As stated previously, Iwo-jima is a volcanic island located in the Pacific Ocean. The surface is covered with dense vegetation and there is no river on the island. The source of sediments is therefore quite limited. Nevertheless, the coast of the island is mostly rimmed by a sandy beach roughly 200 m wide. These observations seem to indicate that upheaval is the only possible mechanism for supplying sediments to the shore of the island.

To confirm this, the authors have checked the relationship between the surface area and the cumulative change in elevation that occurred in the period from 1911 to 1978. The change in elevation was determined from the work done by Kosaka et al (1979).

The results was shown in figure 10, where figures in parentheses indicate the dates of observations. Through this analysis, it was ascertained that there was quite a high correlation between the increase of surface area and the cumulative upheaval height, except for the data prior to 1945. Regression analysis on these data after 1952 indicated that the shore area increased by roughly 270,000 m² per year in this period for an up-

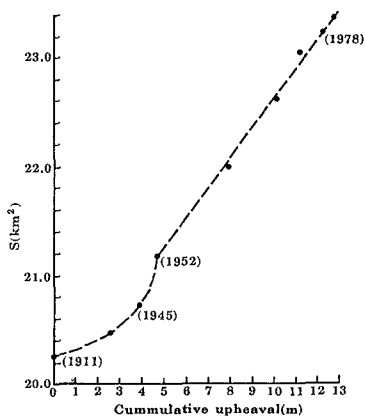


Figure 10 Relationship between the surface area and the cumulative change in elevation

heaval of 1 m. It should be noted that this relationship was found for foreshore areas which had been subject to waves over a certain period.

Next, the increase of the foreshore area due to the upheaval was estimated by applying various upheaval heights and foreshore slopes to the shoreline data of April 24, 1987. The results are shown in figure 11. It should be noted that the increase of foreshore area shown here is the estimated value, without accounting for the effects of waves and currents. If the mean upheaval rate were 30 cm/year, and the mean slope in the surf zone were 1/20, the increase in foreshore area would be roughly 150,000 m²/year. This might be a reasonable value considering the fact that the rate at present is roughly 50,000 m²/year.

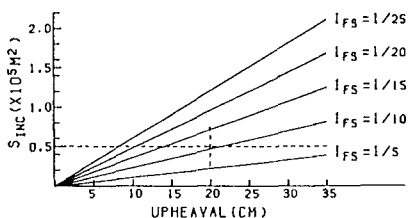


Figure 11 Increase of foreshore area due to the given upheaval height

(5) The response of the foreshore to storm waves

The analyses done so far have revealed that the magnitude and frequency of typhoons would be the governing factors in the variation of the foreshore area in Iwo-jima. It was therefore attempted to predict the short term variation of foreshore transformation due to storm waves generated by typhoons, using numerical models.

Two typhoons were selected for the numerical analyses, whose characteristics are summarized in table 2.

Table 2. Characteristics of typhoons at the times when they approached most closely to Iwo-jima.

Typhoons	Date	Time	P(mb)	R-30kt	Location	DIR
#8911	July.26,1989	00:47	940.0	225 km	350km W	SE
#9813	Aug. 4,1989	14:66	950.0	275 km	370km E	WNW

In this table, R-30kt means the semi-diameter of a circle in which wind velocity is greater than 30 kt. The Location column gives the distance and direction of the center of the typhoon from the island, and the DIR column indicates the direction of the typhoon.

These typhoons were chosen because the authors have the mosaic maps produced from the aerial photographs taken just before and after these typhoons hit the island (see table 1), and it is possible to compare the

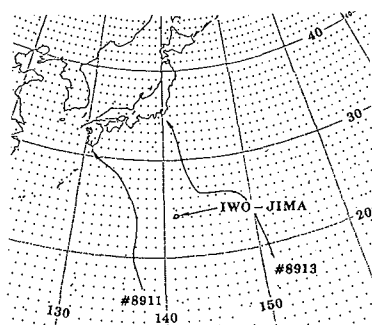


Figure 12 Passage routes of typhoons #8911 and #8913

predicted values with the observed ones.

Figure 12 shows the passage routes of these typhoons. As it is shown in this figure, both typhoons advanced into the NE direction, although typhoon #8911 passed offshore to the west of the island and typhoon #8913 passed to the east.

The numerical analysis consists of a prediction of the offshore waves, calculation of wave transformation and prediction of shoreline variation, as described below.

(a) Prediction of offshore waves generated by typhoons

Prediction of offshore waves was carried out by using the method developed by Goto and Aono (1992) which requires the following steps:

- Determine the typhoon constants at one hour intervals based on the meteorological maps published by Japan Meteorological Agency.
- Compute the wind field around the computational area.
- Select the prediction point of offshore waves at Iwo-jima and calculate the two dimensional energy spectrum $S(f, \theta)$ which is obtained by composing the energy spectrum of waves approaching the prediction point from 16 directions along the respective wave rays.
- Determine the height and period of significant waves at one hour intervals based on the values of $S(f, \theta)$.

(b) Calculation of wave transformation

Wave transformation due to shoaling, refraction and diffraction was calculated as follows using small amplitude wave theory:

- Use a nautical chart published in 1981 by Maritime Safety Agency of Japan for the bathymetry around the island.
- Provide a calculation area around the island in which the depth is less than 100 m. Further, provide a square grid on the calculation area whose length is 50 m.
- Calculate the wave transformation due to shoaling, refraction and diffraction, to determine the magnitude and direction of energy flux at the breaking points. Here, use Goda's breaker formula (1973) as a breaker index.

(c) Prediction of shoreline variation

Shoreline variation was predicted by using a one-line model following the steps shown below:

- Assume the critical water depth for sand movement by waves to be 15 m, and the runup height of waves to be 1 m above mean sea level.
- Compute the longshore sediment transport flux by using the CERC formula, assuming the coefficient of longshore sediment transport rate to be 0.1.
- Assume that the longshore sediment transport flux coming into the computational area through the boundary between adjacent coastal regions to be zero.

Figure 13 shows the time-wise variation of the predicted values of significant wave height, wave period and direction of deep sea

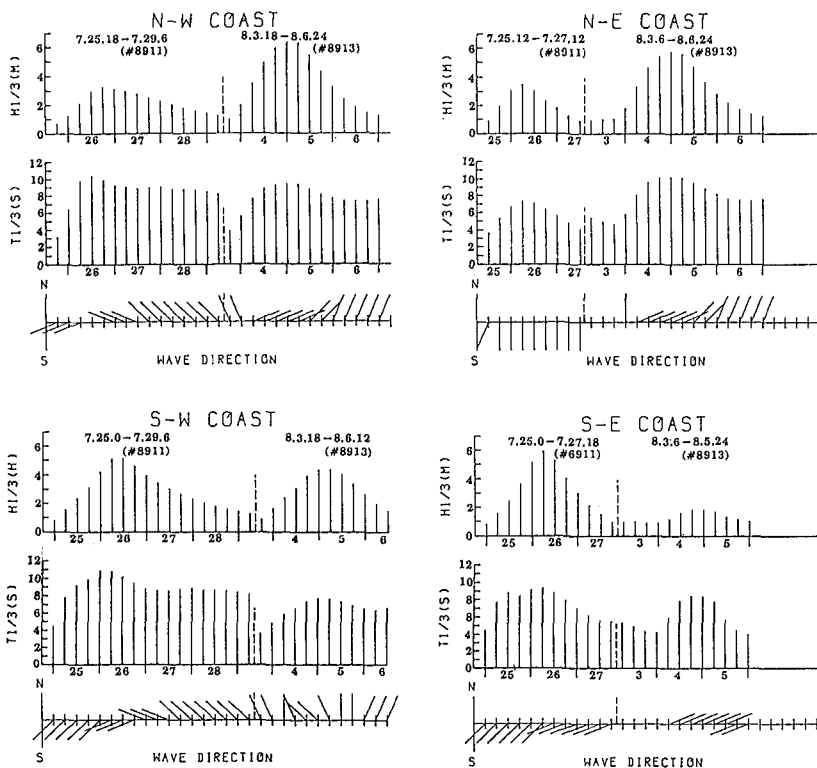


Figure 13 Time-wise variation of the predicted values of significant waves

waves generated by two typhoons. Values after successive intervals of 6 hours are shown in this figure. From this figure, the following facts can be read clearly:

- In the case of typhoon #8911, the direction of generated waves offshore of every subdivided coast at the initial stage is SW. However, it becomes WNW off the west coast, S or WSW off the east coast as the typhoon advances northward. Waves with a peak height of roughly 5.9 m appear off the in S-E coast although wave with peak height of roughly 5.1 m appears in the S-W coast. In the case of typhoon #8913, the wave direction is mainly ENE except for the case of the S-W coast at the initial stage. However, it becomes NNE except for the case of the S-E coast as typhoon advances northward. Waves with a peak height of about 6.4 m appear off the N-W coast, although waves with a peak height of roughly 5.8 m appears off the N-E coast.

Based on these offshore wave predictions, the wave transformation was calculated to determine the breaker characteristics, and

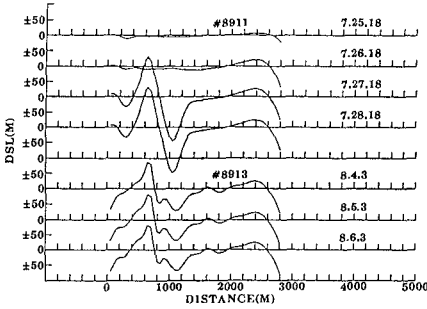


Figure 4(a) Time-wise variation of the shorelines predicted in the S-E coast

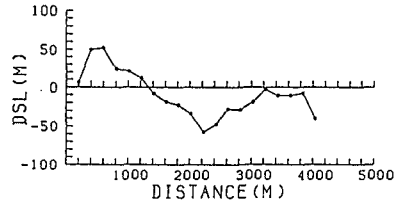


Figure 4(b) Variation of the shoreline observed in the S-E coast in the period between May 15, 1989 and Sep.9, 1989

finally the variation of the shoreline was calculated by the method stated previously. Figure 14(a) shows the time-wise variation of the shorelines predicted for the S-E coast at intervals of 24 hours. On the other hand, figure 14(b) shows the change of the corresponding shoreline determined through the mosaic maps which were made from the aerial photographs taken before and after these typhoons hit the island.

In both figures, the distance shown on the abscissa is that measured southward from the northern boundary on the S-E coast. Here, it should be noted that the predicted variation of the shorelines is based only on the two successive typhoons, although the observed variation of the shoreline is the effect of all waves (including those due to the storm waves during two typhoons) over the period from May 15, 1989 to September 6, 1989. Thus, caution should be exercised in drawing conclusions from a comparison between these two results. However, the numerical analysis clearly indicates that the northern part of the shoreline is considerably eroded by waves with SW direction generated by typhoon #8911 and is restored gradually by waves with NE direction generated by typhoon #8913. Further, the final pattern of the predicted shoreline in figure 14(a) is quite similar to that of the observed shoreline shown in figure 14(b).

Table 3 Comparison of the observed and predicted foreshore areas eroded in summer of 1989

Coasts	S(Observed)	S(Predicted)
N-E	-108,000 m ²	-38,000 m ²
N-W	-63,000 m ²	-54,000 m ²
S-E	-32,000 m ²	-29,000 m ²
S-W	-10,000 m ²	-11,000 m ²

Table 3 summarizes both predicted and observed values of foreshore variation in each subdivided coast. In the case of the N-E

coast, the predicted value of the foreshore variation is quite different from the observed value. This might be caused by the fact that both boundaries of this coast are rocky. However, the model used in this study seems to predict the variation of the foreshore area quite satisfactorily.

4. Conclusions

Foreshore variations in Iwo-jima were investigated by analyzing a series of mosaic maps made from the aerial photographs which had been taken seasonally for the past 4 years since 1978. Analysis was also undertaken on the data of level and cross surveys carried out on the entire beach of the island for the past ten years since 1982. Further, numerical analysis was performed to study the short-term variation of the foreshore area due to storm waves generated by two typhoons which had hit the island in July and August, 1989. The predicted variation of the shorelines was compared with that observed in the corresponding period.

As a result, the following facts were revealed:

- (1) The island is still rising at a rate more than 30 cm/year, although the rate of upheaval increases toward the north.
- (2) The foreshore area is eroded in summer and fall when typhoons often hit the island, but is restored in winter and spring of the following year when waves of roughly 1 m high are predominant.
- (3) The seasonal variation of the foreshore area ranges from 300,000 m² to 600,000 m² per year depending on the magnitude and frequency of the typhoons hitting the island in the year.
- (4) The foreshore area continues to increase currently at a rate of roughly 50,000 m²/year, which is undoubtedly caused by the upheaval of the island.
- (5) A one-line model can be applicable for the prediction of short-term variation of the shoreline caused by storm waves.

References

- Goda, Y. (1973), "On the breaker index of irregular waves", Proc. of the 20th Japanese Conference on Coastal Engineering, JSCE, 571-573 (in Japanese).
- Goto, C. and Aono, T. (1992), "A Spectral Wave Prediction System For A Single Point", Report of the Port and Harbor Research Institute, Ministry of Transport, Japan, Vol. 31, No. 2, 55-73 (in Japanese).
- Kosaka, J. et al (1979), "Investigation Report of the Volcanic Action Ogasawara-Iwo-jima", Santama Office for isolate islands, Tokyo Metropolitan Government, No. 3, 1-89 (in Japanese).
- Sigemura, T. (1986), "Shore Process along the coast of Iwo-jima", Proc. of the 20th ICCE, Chapter 112, ASCE, 1523-1534.
- Tsuji, S., Kuriyama, M. and Tsurumi, T. (1969), "Investigation Report of Ogasawara Islands", Technical note of Geological Institute, Ministry of Construction, Japan, 1-18 (in Japanese).